JEE Journal of Ecological Engineering

Journal of Ecological Engineering, 2026, 27(2), 210–221
https://doi.org/10.12911/22998993/211274
ISSN 2299–8993, License CC-BY 4.0

Received: 2025.09.11
Accepted: 2025.12.15
Published: 2026.01.15

Modified properties of biochar by nano zinc oxide to remove heavy metals (cadmium and lead) from industrial wastewater

Rusol Maki Taleb[1*], Ahmed Khudhair Hassan[1], Mahdi Shanshal Jaafar[1]

[1] Scientific Research Commission, Baghdad, Iraq
* Corresponding author's e-mail: rusol.m.taleb@src.edu.iq

ABSTRACT

In recent decades, the increasing release of industrial effluents has intensified heavy metal contamination in aquatic systems, particularly with lead (Pb^{2+}) and cadmium (Cd^{2+}), both of which are highly toxic, non-biodegradable, and bioaccumulative. Addressing this challenge requires sustainable, cost-effective, and eco-friendly adsorbents. This study reports the green synthesis of ZnO nanoparticles using green tea extract and their subsequent incorporation onto biochar obtained from orange seed biomass that prepared by pyrolysis at 500 OC. The composite was systematically characterized using field emission scanning electron microscopy (FESEM), X-ray diffraction (XRD), Fourier-transform infrared spectroscopy (FTIR), dynamic light scattering (DLS), and Zeta potential analyses. Results confirmed the successful embedding of ZnO nanoparticles within the biochar matrix, yielding a highly crystalline hybrid with abundant surface functional groups. Batch adsorption experiments were performed to evaluate the removal efficiency of Pb^{2+} and Cd^{2+} under varying parameters, including pH, dosage, initial concentration, and temperature. Optimal conditions (pH 7, 2 g adsorbent dosage, 15 mg/L initial ion concentration and 45 OC) achieved removal efficiencies of 99.1% for Pb^{2+} and 98.2% for Cd^{2+}. Adsorption behavior was best described by the Langmuir isotherm model, with high correlation coefficients ($R^2 = 0.9943$ for $Pb^{2+}$and 0.9912 for Cd^{2+}), indicating monolayer adsorption on homogeneous surfaces. The findings demonstrate that ZnO nano composites –biochar derived from agricultural waste represent an efficient and sustainable adsorbent for heavy metal removal, aligning with green chemistry principles and offering a promising alternative for wastewater treatment applications.

Keywords: heavy metals, biochar, zinc oxide nanoparticles, adsorption, green synthesis, wastewater treatment.

INTRODUCTION

In recent decades, industrial expansion has substantially contributed to the contamination of water resources with heavy metals, especially lead (Pb) and cadmium (Cd). These metals are highly toxic, persistent in aquatic ecosystems, and capable of bioaccumulation, posing significant ecological and health risks. Prolonged exposure to Pb and Cd has been linked to kidney damage, neurological disorders, and potential carcinogenic effects (Mitra et al., 2022). Major industrial activities, such as battery manufacturing, metal plating, and pigment production, are key sources of heavy metal pollution in water, raising global concerns about the efficiency and sustainability of existing wastewater treatment methods (Odumbe et al., 2023). Among the various strategies for removing heavy metals from wastewater, adsorption stands out for its simplicity, efficiency, and cost-effectiveness. Techniques like chemical precipitation, coagulation, ion exchange, and membrane filtration have been widely applied, but adsorption has proven to be particularly promising due to its high removal efficiency and ease of reuse. Recently, research has increasingly focused on developing environmentally friendly and highly efficient adsorbents. Biochar, a carbon-rich material produced by pyrolysis of biomass the with oxygen isolated from the environment, has gained attention for its porous structure, large surface area, and functional groups that facilitate pollutant removal (Bayar et al., 2024). However, pristine biochar often shows limited capacity for certain heavy metals, prompting modifications to enhance its performance. Incorporating

nanoparticles into biochar has emerged as a highly effective approach. These nanoparticles offer a high surface-to-volume ratio, chemical stability, and active sites that improve interaction with metal ions (Ahuja et al., 2022). When integrated with biochar, these nanocomposites exhibit synergistic effects that significantly improve the adsorption capacity for Pb and Cd. The modified biochar acts not only as a support matrix but also as a co-active agent, providing a robust and multifunctional adsorbent system (Tan et al., 2016). Recent studies have reported that such biochar-nanocomposites offer a range of benefits, including improved adsorption kinetics, higher selectivity toward specific metal ions, reusability, and compatibility (Zhang et al., 2025). These materials follow the core ideas of green chemistry and sustainable environmental practices. They offer an eco-friendly alternative to traditional chemical treatments, which often lead to secondary pollution. While good progress has been made, there is still a clear need to better understand how the structure of these nanocomposites affects their function, and how they perform under different environmental conditions. Factors like the type of biomass used, the synthesis method, and the amount of nanoparticles added all play a role in shaping their adsorption behavior (Gul et al., 2021). Therefore, this research aimed at a modification of the biochar made from orange seeds with zinc oxide nanoparticles to enhance its ability to remove Pb and Cd from industrial wastewater, with a particular emphasis on optimizing material properties and adsorption efficiency under variable operational parameters.

EXPERIMENTAL METHODS

Biochar preparation

Orange seeds were collected, washed, and air-dried, then ground and subjected to pyrolysis at 500 °C for 2 hours in environment isolated oxygen to produce biochar. The resulting biochar was allowed to cool, washed with distilled water, dried at 90 °C, sieved to particles <100 μm, and stored in an airtight container.

Green synthesis of ZnO nanoparticles

The green tea extract was prepared by boiling tea leaves in distilled water at 80 °C for one hour, filter the solution. Zinc sulfate ($ZnSO_4 \cdot 7H_2O$) was dissolved in distilled water. The zinc solution was mixed with tea extract and following the complete addition of the extract to the zinc salt solution, the pre-prepared biochar – derived from orange seed biomass – was introduced into the reaction mixture. Stirring was carried out at 70 °C for 2 hour until precipitation forms. Centrifuge, wash, dry, and calcination the ZnO at 300 °C to obtain nanoparticles.

Regeneration of the biochar-ZnO composite

The desorption of Pb^{2+} and Cd^{2+} from ZnO-modified biochar was evaluated using HCl and $CaCl_2$ solutions. After adsorption of 15 mg/L Pb^{2+} and Cd^{2+}, the suspensions were centrifuged for 10 min and filtered. The loaded biochar was then regenerated by shaking in 10% HCl for 30 min or in 0.1 M $CaCl_2$ for 30 min. Afterwards, the desorbed biochar was dried in an oven at 80 °C for 1 h. This adsorption–desorption procedure was repeated three times, and the removal efficiencies of Pb^{2+} and Cd^{2+} were calculated after each cycle.

Characterization of the adsorbent

To understand the physicochemical properties of the synthesized adsorbent and evaluate its potential for heavy metal removal, several analytical techniques were employed. These techniques provided information on the structural, morphological, functional, and surface charge characteristics of the material:

Zeta potential measures the surface charge of particles in a liquid and indicates the stability of the colloidal dispersion. Dynamic light scattering (DLS) measures the particle size distribution in a suspension by analyzing how light scatters off moving particles, using the Brownian motion to calculate their hydrodynamic diameter. X-ray diffraction (XRD) was used to identify the crystalline phases and assess the degree of crystallinity in the nan composite. Scanning electron microscopy (SEM) provided visual insight into the surface morphology and particle size distribution of the adsorbent.

Fourier-transform infrared spectroscopy (FTIR) was utilized to detect the functional groups present on the surface, which play a key role in the adsorption process. Zeta potential analysis was carried out to determine the surface charge of the adsorbent and its stability in

aqueous media, which influences the electrostatic interactions with metal ions.

Atomic absorption spectroscopy (AAS) was used to measure the concentrations of lead (Pb^{+2}) and cadmium (Cd^{+2}) ions before and after adsorption, allowing for the calculation of removal efficiency and adsorption capacity. These characterization methods collectively help in understanding how the structural and chemical features of the material contribute to its adsorption performance.

Parameters of adsorption

In order to evaluate the adsorption performance of the prepared biochar-based nano composite, a series of batch experiments were conducted under varying conditions. Key operational parameters were selected based on their known influence on adsorption behavior. These include: Solution pH, which affects the surface charge of the adsorbent and the speciation of metal ions in solution, Adsorbent dosage, which determines the availability of active sites for metal ion uptake, Initial concentrations of Pb^{+2} and Cd^{+2} ions, which help assess the adsorption capacity of the material at different loading levels, as well as Temperature, which provides insight into the thermodynamic nature of the adsorption process and helps determine whether it is endothermic or exothermic. By systematically varying these parameters, the study aimed to better understand how each factor contributes to the removal efficiency of lead and cadmium ions from aqueous solutions using the synthesized composite.

Isotherm studies

Understanding the mechanism of adsorption requires examining how adsorbate molecules interact with the surface of the adsorbent under different conditions. To do this, adsorption isotherm models are used to describe the relationship between the amount of adsorbate retained on the surface and its concentration in the solution at equilibrium. Among the most widely used models: the Langmuir isotherm assumes monolayer adsorption on a uniform surface with a finite number of identical sites, with no interaction between adsorbed molecules (Ganguly et al., 2020) as illustrated by equation (1) below:

$$\frac{C_e}{Q_e} = \frac{C_e}{Q_m} + \frac{1}{Q_m b} \quad (1)$$

The Freundlich isotherm is an empirical model that describes adsorption on heterogeneous surfaces, allowing for multilayer formation and varying affinities of sites (Dagmawi and Mekibib, 2013) mathematically expressed as follows:

$$lnQ_e = lnk_f + \frac{1}{n} lnC_e \quad (2)$$

Removal efficiency (R %) was determined according to:

$$R\,\% = \frac{C_o - C_e}{C_0} \times 100 \quad (3)$$

Equilibrium adsorption capacity (Qe) was calculated using:

$$Q_e = \frac{(C_o - C_e) \times V}{M} \quad (4)$$

where: C_e – is the initial concentration of Pb^{2+} or Cd^{2+} in the solution (mg/L), C_o – is the equilibrium concentration of the ion remaining in the solution (mg/L), Qe – is the amount of Pb^{2+} or Cd^{2+} adsorbed per unit mass of adsorbent (mg/g), V – is the volume of the solution used in the experiment (L), M – is the mass of the adsorbent used (g), Qm – Maximum adsorption capacity of the adsorbent (mg/g), based on the Langmuir model: Langmuir constant, which reflects the affinity of the binding sites (L/mg), Kf – Freundlich constant related to adsorption capacity at equilibrium (mg/g), n – Freundlich constant indicating the intensity or favorability of the adsorption process.

RESULTS AND DISSECTION

Analysis of SEM

Figure 1 shows the FESEM image of biochar-coated ZnO nanoparticles at 120,000× magnification. The surface appears heterogeneous, with fine ZnO nanostructures overlaid by irregular biochar deposits (He and Wang et al., 2021). The wrinkled and amorphous carbon phase is evident in multiple regions, particularly where agglomeration has occurred. These features align with biochar–metal oxide composites, where carbonaceous coatings enhance surface roughness and improve interaction with target pollutants. The overall morphology supports the effective anchoring of biochar onto ZnO, which may enhance functional properties such as adsorption capacity.

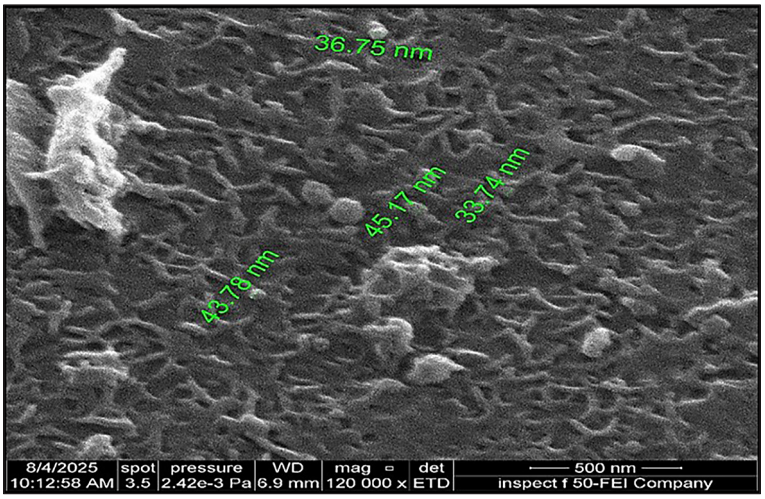

Figure 1. Image of SEM for ZnO nanoparticles with biochar

Analysis of XRD

The crystalline structure of the synthesized ZnO nanoparticles was examined using X-ray diffraction (XRD), as illustrated in Figure 2. The diffraction pattern exhibited a series of sharp and well-defined peaks at 2θ values of approximately 31.7°, 34.4°, 36.2°, 47.5°, 56.6°, 62.8°, and 67.9°, which correspond to the (100), (002), (101), (102), (110), (103), and (112) crystal planes, respectively. These peaks are in good agreement with the standard hexagonal wurtzite structure of ZnO, as per JCPDS card no. 36-1451, confirming the formation of a single-phase crystalline material (Chowdhury et al., 2023).The intensity and sharpness of the diffraction peaks indicate a high degree of crystallinity. No secondary phases or impurity-related peaks were detected, suggesting the successful synthesis of pure ZnO nanoparticles (Grace et al., 2023). Furthermore, the dominance of the (101) peak suggests a preferred orientation in that direction. These structural characteristics are favorable for applications in adsorption processes, as the high crystallinity and purity enhance surface reactivity as well as stability under aqueous conditions (Mondal, 2024). X-ray diffraction (XRD) analysis of the ZnO-biochar composite reveals distinct crystalline peaks corresponding to ZnO, with primary reflections observed at 2θ ≈ 31.8°, 34.4°, and 36.2°, which match the (100), (002), and (101) planes of hexagonal wurtzite ZnO, according to JCPDS Card No. 36-1451 (Golhar (2024). A broad background signal in the 10–30° region indicates the presence of amorphous carbon from biochar, suggesting that ZnO retained its crystallinity while being embedded within a non-crystalline carbon matrix (Goncalves et al., 2022). The pattern confirms successful synthesis of the ZnO-biochar hybrid with preserved crystalline structure of ZnO and proper dispersion within the amorphous matrix.

Analysis of FTIR

FTIR Analysis of ZnO Nanoparticles: The FTIR spectrum of ZnO nanoparticles in Figure 3 exhibits characteristic absorption bands that indicate the presence of specific functional groups associated with zinc oxide. A broad band around 3400–3500 cm^{-1} is observed, which corresponds to the stretching vibrations of hydroxyl (–OH) groups (Adamu et al., 2024). This can be attributed to adsorbed water molecules or surface –OH groups on the ZnO nanoparticles, which is common due to their high surface area and hygroscopic nature. A sharp and well-defined peak in the region below 500 cm^{-1}, typically around 450–480 cm^{-1}, is attributed to the Zn–O stretching vibrations, confirming the successful formation of zinc oxide nanoparticles. The absence of significant peaks related to organic contaminants suggests that the nanoparticles are relatively pure (Zahra et al., 2022). In comparison, the FTIR spectrum of the ZnO–biochar composite exhibits several notable changes. Firstly, the broad –OH stretching band near 3400 cm^{-1} is still present, but slightly shifted and less intense, indicating interactions between ZnO and the functional groups on the biochar surface. New bands emerge in the region of 1600–1700 cm^{-1}, which are attributed to C=O stretching vibrations of carboxylic or

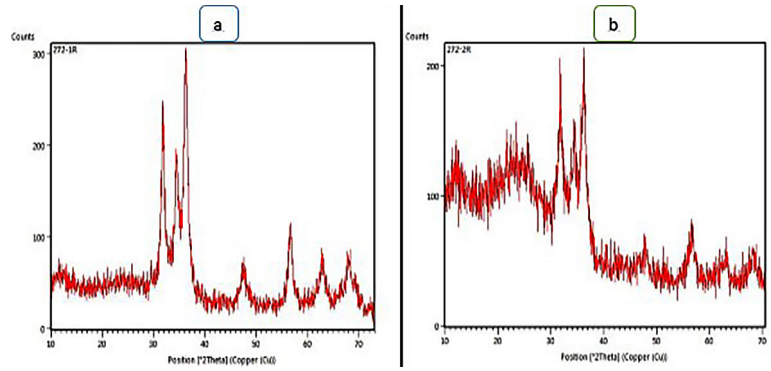

Figure 2. Spectrum of X-ray diffraction for (a) ZnO nano particals (b) ZnO with biochar

carbonyl groups, confirming the presence of biochar (Saeednia et al., 2024). Additionally, peaks in the region 1000–1200 cm^{-1} correspond to C–O stretching of alcohols, ethers, or esters, further supporting the biochar incorporation (Gurusamy et al., 2025). Importantly, the ZnO peak remains evident in the composite, but with reduced intensity and slight shifts, indicating physical interaction or weak chemical bonding between ZnO and the biochar. These spectral changes confirm the successful functional integration of ZnO nanoparticles within the biochar structure (Dawood et al., 2025). The FTIR analysis confirms the formation of pure ZnO nanoparticles and the successful development of a ZnO–biochar composite, with distinct spectral features representing both components. The observed shifts and new functional group appearances indicate strong interaction between ZnO and biochar, enhancing the potential of the composite for adsorption or catalytic applications.

Zeta potential and dynamic light scattering (DLS)

The measured zeta potential of the ZnO-biochar in Figure 4 sample is -55.86 mV, indicating a highly stable colloidal suspension. A high negative zeta potential suggests strong electrostatic repulsion between particles, which prevents aggregation and enhances dispersion in aqueous solutions. This stability is beneficial for applications in water treatment, where good dispersion of nanoparticles ensures effective surface contact with pollutants (Nagaraju et al., 2023). The high magnitude of the zeta potential also implies that the biochar surface is rich in negatively charged functional groups, likely contributed by oxygen-containing groups such as –COOH and –OH, which are known to enhance adsorption capabilities. Moreover, the integration with ZnO may further contribute to the surface charge through ionization of surface hydroxyl groups. In conclusion, the ZnO-biochar nanocomposite demonstrates excellent colloidal stability, making it a promising candidate for environmental applications, particularly in adsorption and photocatalysis processes.

DLS interpretation and adsorption behavior of biochar-coated ZnO nanoparticles

The DLS results of biochar-coated ZnO nanoparticles showed particle sizes ranging 106 nm with a PDI of 0.312, indicating moderate polydispersity and partial aggregation. Loading biochar onto the surface of ZnO nanoparticles introduces additional functional groups, such as –OH, –COOH, and –C=O, which significantly enhance the adsorptive properties of the material. The biochar coating not only stabilizes the ZnO nanoparticles but also improves their interaction with pollutants by increasing surface roughness, porosity, and chemical affinity. This hybrid structure combines the high reactivity of ZnO with the surface functionality of biochar, creating a synergistic adsorbent that is more effective for capturing heavy metals and organic contaminants from aqueous media.

Optimization of pH

The pH of the solution is one of the most critical factors influencing the adsorption of heavy metal ions. In this study, the effect of pH was investigated over a range of values (3 to 9) to determine the optimal condition for the removal of Cd^{+2} and Pb^{+2} ions in Figure 5. The pH affects both the surface charge of the adsorbent and the chemical speciation of the metal ions (Heo et al., 2022). Optimum removal at

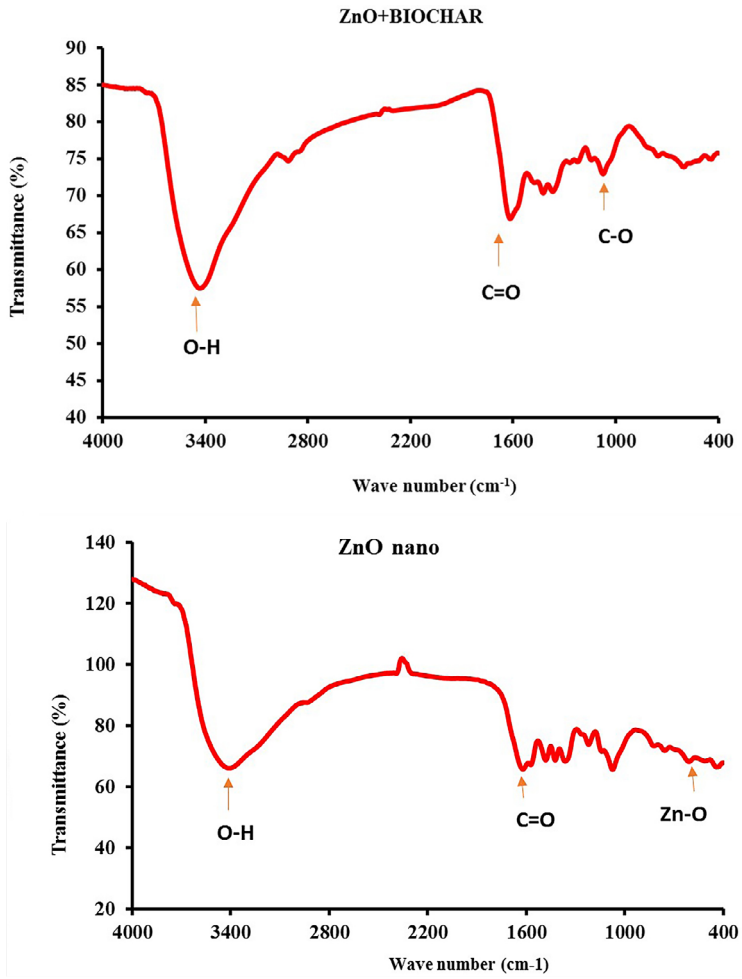

Figure 3. Spectrum of FTIR for ZnO nanoparticles and ZnO with biochar

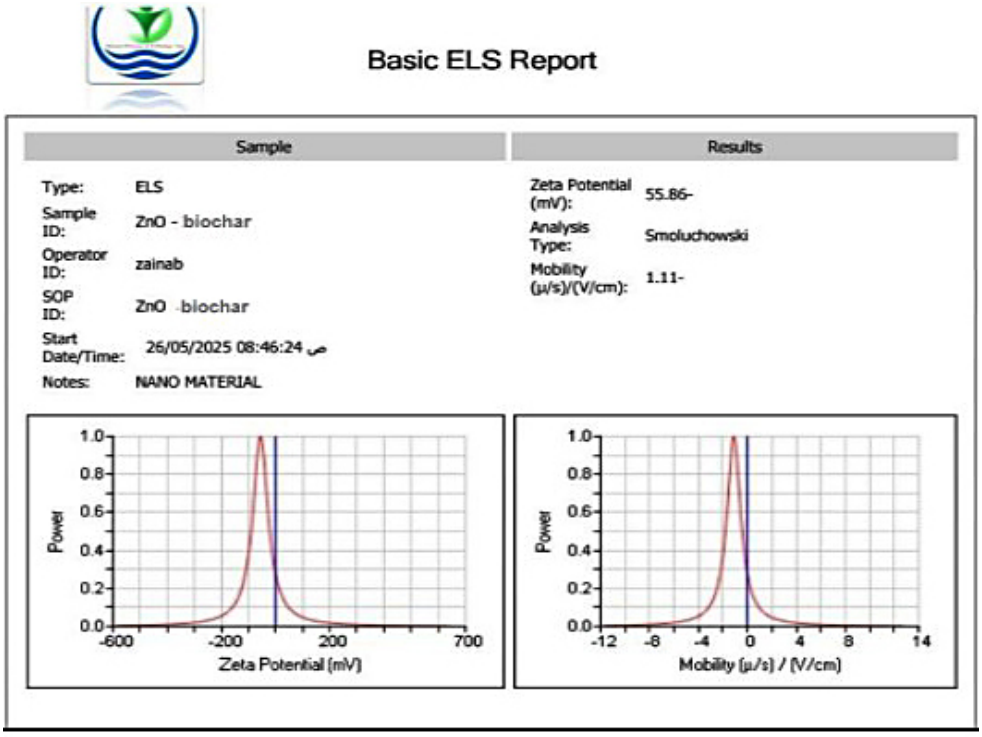

Figure 4. Analysis of Zeta potential for ZnO with biochar

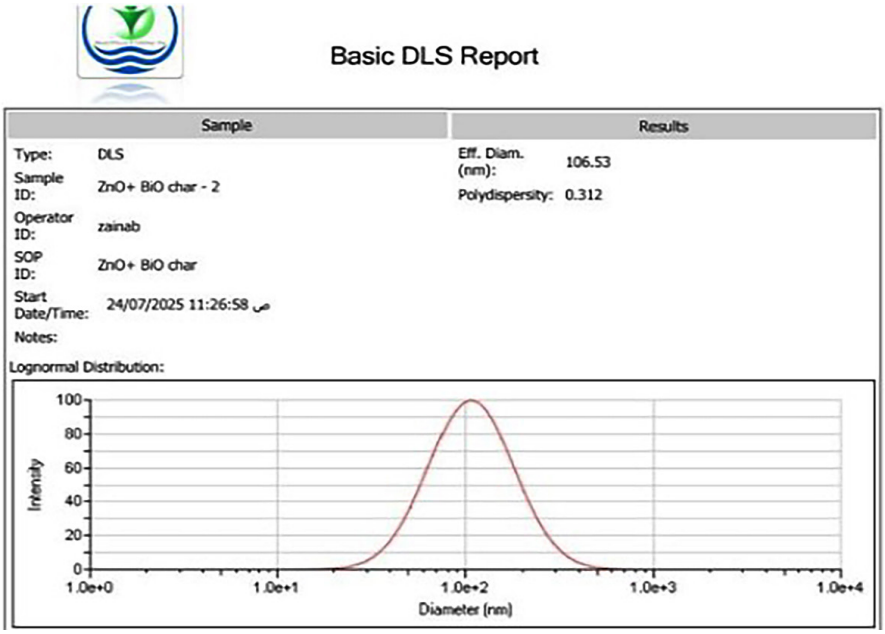

Figure 5. Analysis of Dynamic light scattering for ZnO with biochar

pH 7 reached 95%, 90% for lead and cadmium respectively at concentrations of Pb^{+2} and Cd^{+2} (10 mg/L each). The pH of solutions was adjusted to 3, 5, 7, and 9 using HCl/NaOH and dose of adsorbent (1 g in 1000 mL). They were shaken for a constant time (60 minutes) at room temperature with speed 200 rpm. Optimum pH reached 7 (Figure 6). At lower pH levels, the presence of excess H^+ ions competes with metal ions for available adsorption sites, resulting in lower removal efficiency. As the pH increases, the competition decreases and the adsorbent surface becomes more negatively charged, enhancing the electrostatic attraction toward positively charged metal ions. However, at very high pH values, metal ions may precipitate as hydroxides rather than adsorb, which can interfere with accurate adsorption measurement (Ramutshatsha-Makhwedzha et al., 2022).

Adsorbent dose

Identifying this optimum dosage is essential for ensuring cost-effective and efficient treatment. The pH was fixed at 7 and contact time at 60 min. Different doses were used (0.5, 1, 1.5, 2 and 2.5 g per 1000 mL), with concentration of Pb, Cd amounting to 10 mg/L, shaking speed 200 rpm, filtrated and removal efficiency was measured. The goal was to determine the optimal dosage that achieves maximum removal efficiency of Cd^{+2} and Pb^{+2} ions. Increasing the adsorbent dose generally enhances the removal efficiency due to the greater number of available active sites for adsorption, as shown in Figure 7 (Chigova and Mudono, 2022). However, after reaching 2 g a certain point, further increase in dosage may not significantly improve removal, possibly due to

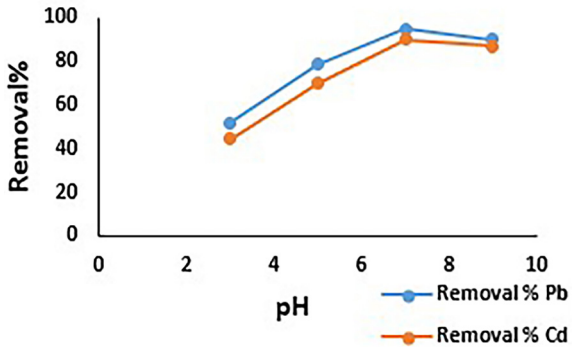

Figure 6. As shown effect pH on adsorption

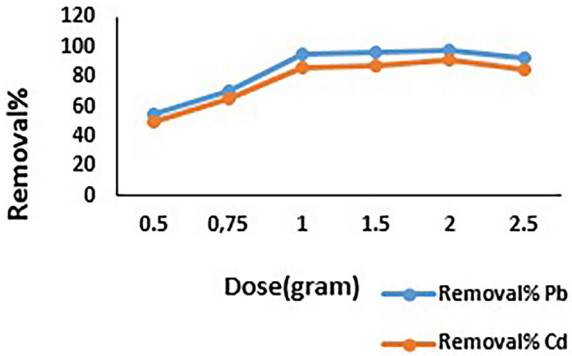

Figure 7. Illustrated effect adsorbent dose on adsorption

particle aggregation or site saturation (Padmavathy et al., 2016). The optimum removal for lead and cadmium was 97.5% and 91.9%, respectively, at 2 g dose.

Initial metal concentration effect

This study helps in understanding the adsorption behavior under varying pollution concentrations and contributes to the design of treatment systems for real wastewater conditions. Different Pb^{+2} and Cd^{+2} concentrations were used (5, 10, 15, 20, 25, and 30 mg/L). All other parameters were constant. Lower removal was observed at 5 and 10 mg/L, followed by a highest at 15 mg/L 98.4% and 94.5% for Pb and Cd respectively; then, a gradual decline at higher concentrations illustrated in Figure 8. This behavior may be attributed to limited interaction between metal ions and active sites at low concentrations. At 15 mg/L, optimal adsorption occurred due to better surface interaction. Beyond this point, site saturation likely reduced the available binding capacity, leading to decreased removal efficiency (Cherono et al., 2021).

Adsorption temperature

After optimizing the pH adsorbent dose ad initial metal concentration, the next step in this study is to examine the effect of temperature on the adsorption efficiency of cadmium and lead illustrated in Figure 9. This involves conducting batch adsorption experiments at different temperature (25, 35, 45 and 55 °C) while keeping all other conditions constant. Optimum removal when temperature 45 °C 99.1% for Pb and 98.2% for cadmium. The observed decrease in removal efficiency beyond 45 °C may also be attributed to weakening interactions between metal ions and the functional groups on the adsorbent surface. At high concentrations, excessive loading of Pb^{+2} and Cd^{+2} ions can lead to partial desorption due to repulsive forces and overcrowding of binding sites. The saturation of active sites at high concentrations may disrupt the stability of adsorbate-adsorbent bonds, causing some ions to detach and re-enter the solution. This results decrease in removal efficiency (Jawad and Naife, 2022).

Regeneration of the biochar-ZnO composite

As shown in Table 2, HCl and $CaCl_2$ promoted desorption mainly through the high concentration of H^+ and Ca^{2+}ions ions readily replaced the adsorbed metal cations via ion exchange (Abedi et al., 2018). In comparison, $CaCl_2$ was more effective than which competed with Pb^{2+} and Cd^{2+} for binding sites on the biochar surface (Coelho et al., 2014). After three adsorption-desorption cycles, the composite maintained high removal efficiency with only a slight decline, demonstrating its potential for repeated use in wastewater treatment.

Isotherm models

The adsorption behavior of lead and cadmium ions onto the biochar surface modification with ZnO nano was well described by the Langmuir isotherm model in Figure 10, as evidenced by the high correlation coefficients obtained for both metals. For lead (Pb^{+2}), the model exhibited an excellent fit with an R^2 value of 0.9943, while cadmium (Cd^{+2}) showed a similarly strong fit with an R^2 of 0.9912. These values indicate that the adsorption process

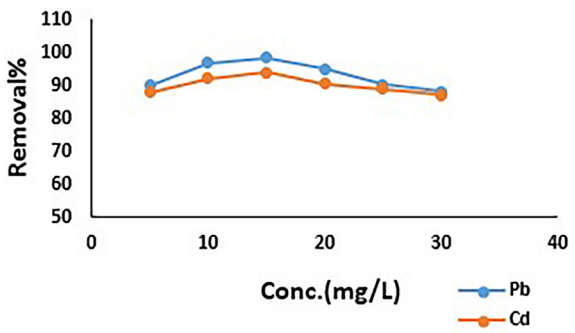

Figure 8. Illustrated effect initial ion concentration on adsorption

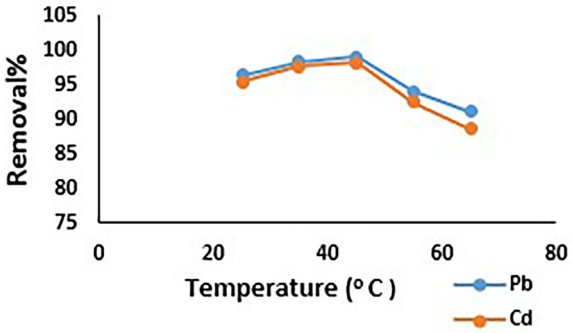

Figure 9. As shown effect temperature on adsorption

likely involves monolayer coverage on a uniform surface. The maximum adsorption capacity (Q_m) shown in Table 1 was slightly higher for lead (38.91 mg/g) compared to cadmium (36.49 mg/g), suggesting a marginally greater uptake potential of the biochar for Pb under the tested conditions. Furthermore, the Langmuir constant (k), which reflects the affinity of the adsorbent for the adsorbate, was found to be 4.1284 L/mg for lead and 3.7555 L/mg for cadmium confirming a stronger interaction between the ZnO nano with biochar and Pb^{+2} ions. Additionally, the separation factor (R_L) is commonly used to assess the favorability of the adsorption process. An R_L value equal to zero suggests an irreversible adsorption behavior, while a value of one indicates a linear adsorption pattern. When R_L falls between zero and one, the process is considered favorable. In contrast, values greater than one reflect an unfavorable adsorption interaction (Al-Hermizy et al., 2025). The dimensionless separation factor (R_L), which provides insight into the favorability of the adsorption process, ranged between 0.2678 and 0.6459 for Pb^{+2}, and between 0.2801 and 0.6605 for Cd^{+2}, across the studied concentration range. The fact that all RL values lie between 0 and 1 further supports that the adsorption of both metals is favorable and efficient. In contrast, Figure 11 shows the Freundlich model, which assumes a heterogeneous multilayer adsorption, exhibits lower R^2 values, particularly for Pb^{+2} (0.834), while Cd^{+2} achieves a higher R^2 of 0.921. The Freundlich constant (Kf) indicates a higher adsorption capacity for Pb^{+2} (9.01) compared to Cd^{+2} (7.46), whereas the heterogeneity factor (1/n) exceeds unity for both metals 2.5 for $Pb^{+2}$and 2.0 for Cd^{+2}, suggesting possible cooperative adsorption or multilayer interactions. Comparing the two models, it is evident that although Pb^{+2} demonstrates higher uptake capacity (K_f) under the studied conditions, its adsorption behavior is more complex, as reflected by the lower Freundlich R^2. Conversely, Cd^{+2} adsorption aligns better with the Freundlich assumptions,

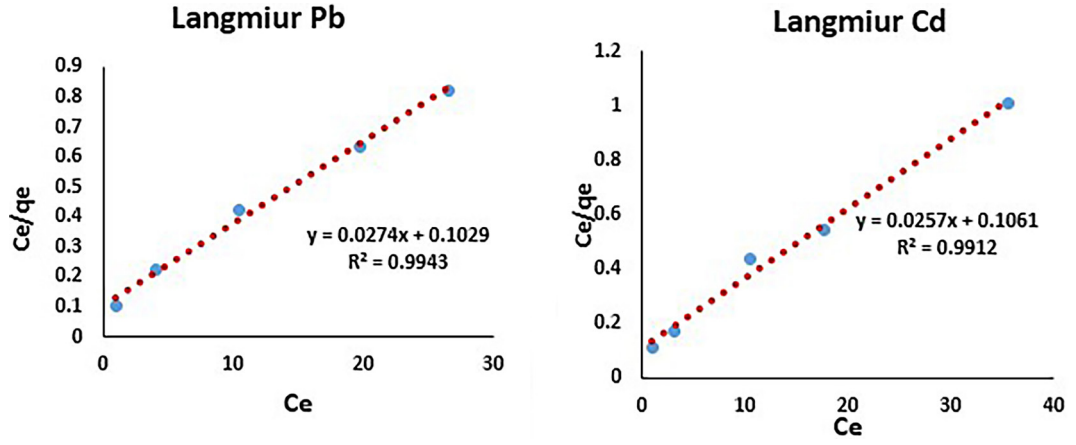

Figure 10. Shown Langmuir model for adsorption Pb and Cd on surface of ZnO nano particle with biochar

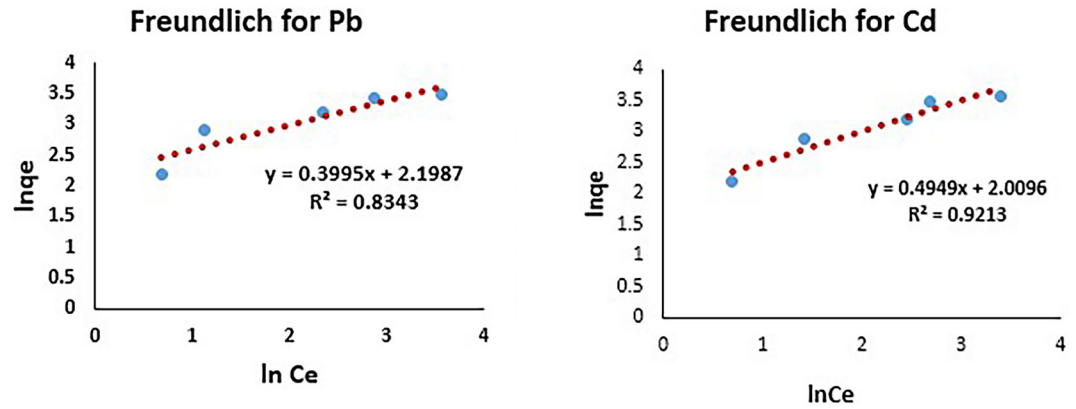

Figure 11. Shown Freundlich model for adsorption Pb and Cd on surface of ZnO nano with biochar

Table 1. Explain value of Langmuir and Freundlich model for ZnO with biochar

Langmuir model				Freundlich model			
ZnO + biochar	R^2	K_L	q_{max}	q_{exp}	R^2	K_f	1/n
Pb	0.9943	3.755	38.9	36.5	0.8343	9.01	2.50
Cd	0.9912	4.128	36.49	35.15	0.9213	7.46	2.02

Table 2. The value of generation of Biochar-ZnO composite after three cycles

Type of desorption material	Removal Cd from Biochar/ZnO	Removal Pb from Biochar/ZnO
$CaCl_2$	94.15%	92%
HCl	86%	82.1%

Table 3. Comparison of the Pb+2 and Cd+2 removal efficiency of different biochar material

Adsorbents	Catalyst concentration	Contaminants concentration	Removal efficiency	Reference
Mg-modified straw biochar	0.4 g	Pb^{+2} 10 mg/L; Cd^{+2} 10 mg/L	96.57% for Pb 93.37% for Cd	Li, 2023
Fruit peel of dragon fruit	0.25 g	Pb^{+2} 100 mg/L; Cd^{+2} 20 mg/L	97.8% for Pb 97.1% for Cd	Wattanakornsiri et al., 2022
Sesbania bispinosa biochar (SBBC)/ copper oxide nanoparticles composite	1 g	Pb^{+2} 25 mg/L Cd^{+2} 25 mg/L	98.7% for Pb 95.5% for Cd	Imran et al., 2023
Modification of coconut shell-based activated carbo	1 g	Pb^{+2} 5 mg/L Cd^{+2} 5 mg/L	92% for Pb 98% for Cd	Deng et al., 2021
Orange seeds biochar /ZnO nanoparticle composite	2 g	Pb^{+2} 15 mg/L Cd^{+2} 15 mg/L	99.1% for Pb and 98.2 for Cd	This study

indicating a more uniform distribution across heterogeneous sites, albeit with slightly lower capacity. Overall, the Langmuir model provides a superior description for both metals, confirming monolayer adsorption as the predominant mechanism, while the Freundlich parameters offer additional insight into surface heterogeneity and adsorption intensity (Figure 11).

Table 3 compares of the Pb(II) and Cd(II) removal efficiency of different biochar materials reported. The results indicate significant influences on the removal efficiency.

CONCLUSIONS

The ZnO-biochar nano composite exhibits enhanced adsorption performance for Pb^{+2} and Cd^{+2}, attributed to its tailored surface properties. SEM analysis. The surface appears heterogeneous, with fine ZnO nanostructures overlaid by irregular biochar deposits, while the incorporation of biochar introduced additional functional groups that act as active sites, further promoting metal binding. Zeta potential measurements (-55 mV) indicate a negatively charged surface, enhancing electrostatic attraction toward cationic metal ions. The adsorption behavior follows the Langmuir model, suggesting predominantly monolayer adsorption on homogeneous sites. Overall, the synergistic effect of ZnO nanoparticles and biochar provides a highly efficient and versatile adsorbent for heavy metal removal. Overall, the synergistic effect of ZnO nanoparticles and biochar provides a highly efficient and versatile adsorbent for heavy metal removal. While the material demonstrated excellent performance, a few aspects deserve attention in future work. Its synthesis is more elaborate than that of raw biochar, and its long-term behavior under real wastewater conditions requires further validation. Minor loss of capacity upon reuse and the need for scale-up optimization should also be considered, though these represent opportunities for refinement, rather than major limitations. Importantly, regeneration studies revealed that the composite can be reused for at least three cycles with minimal loss of capacity, particularly when regenerated with $CaCl_2$ solution. This reusability further supports its promise as a cost-effective and sustainable adsorbent.

Acknowledgment

The authors would like to express their sincere gratitude to the Scientific Research Commission for their continuous support and encouragement. This study would not have been possible without their valuable guidance and dedication to advancing scientific research in Iraq.

REFERENCES

1. A. Dawood, E., Mohammed, T. J., Al-Timimi, B. A., H. Khader, E. (2025). Photocatalytic degradation of petroleum wastewater using ZnO-loaded pistachio shell biochar: A sustainable approach for oil and COD removal. *Reactions*, *6*(3), 38. https://doi.org/10.3390/reactions6030038.
2. Adamu, T. B., Mengesha, A. M., Kebede, M. A., Bogale, B. L., Kassa, T. W. (2024). Facile biosynthesis of zinc oxide nanoparticles (ZnO NPs) using *Lupinus albus* L (Gibto) seed extract for antibacterial and photocatalytic applications. *Results in Chemistry*, *10*, 101724. https://doi.org/10.1016/j.rechem.2024.101724
3. Ahuja, R., Kalia, A., Sikka, R., P, C. (2022). Nano modifications of biochar to enhance heavy metal adsorption from wastewaters: a review. *ACS omega*, *7*(50), 45825–45836. https://doi.org/10.1021/acsomega.2c05117
4. Al-Hermizy, S. M. M., Awadh, H. A., Abbas, M. N. (2025). Biosorption technique using water hyacinth plant as an effective and sustainable approach for treating oil refinery waste: Vanadium element as a case study. *Journal of Ecological Engineering, 26*(6), 251–272. https://doi.org/10.12911/22998993/202658
5. Bayar, J., Ali, N., Dong, Y., Ahmad, U., Anjum, M. M., Khan, G. R., Ali, L. (2024). Biochar-based adsorption for heavy metal removal in water: a sustainable and cost-effective approach. *Environmental geochemistry and health*, *46*(11), 428. http://doi:10.1007/s10653-024-02214-w
6. Cherono, F., Mburu, N., Kakoi, B. (2021). Adsorption of lead, copper and zinc in a multi-metal aqueous solution by waste rubber tires for the design of single batch adsorber. *Heliyon*, *7*(11). https://doi.org/10.1016/j.heliyon.2021.e08254.
7. Chigova, J. T., Mudono, S. (2022). Adsorption of chromium (VI) using nano-ZnO doped scrap tire-derived activated carbon. *Journal of Geoscience and Environment Protection*, *10*(9), 121–135. https://doi.org/ 10.4236/gep.2022.109008
8. Chowdhury, A. S., Islam, M. M., Ghosh, A. (2024, June). Green Synthesis and Characterization of ZnO Nanoparticles from the Extract of *Tagetes erecta* Leaves. In *Proceedings of the 14th International Conference on Mechanical Engineering (ICME 2023)*. https://doi.org/10.2139/ssrn.4859507
9. Deng, Z., Sun, S., Li, H., Pan, D., Patil, R. R., Guo, Z., Seok, I. (2021). Modification of coconut shell-based activated carbon and purification of wastewater. *Advanced Composites and Hybrid Materials, 4*(1), 65–73. https://doi.org/10.1007/s42114-021-00205-4
10. Ganguly, P., Sarkhel, R., Das, P. (2020). Synthesis of pyrolyzed biochar and its application for dye removal: Batch, kinetic and isotherm with linear and non-linear mathematical analysis. *Surfaces and Interfaces*, *20*, 100616. https://doi.org/ 10.1016/j.surfin.2020.100616
11. Golhar, N. P. (2024). Synthesis and structural characterizations of ZnO@ NiO nanocomposite. *IJSAT-International Journal on Science and Technology*, *15*(1). https://doi.org/ 10.5281/zenodo.15282087
12. Goncalves, N. P., Lourenco, M. A., Baleuri, S. R., Bianco, S., Jagdale, P., Calza, P. (2022). Biochar waste-based ZnO materials as highly efficient photocatalysts for water treatment. *Journal of Environmental Chemical Engineering*, *10*(2), 107256. https://doi.org/ 10.2139/ssrn.3979448
13. Grace, M. A. L., Rao, K. V., Anuradha, K., Jayarani, A. J., Rathika, A. (2023). X-ray analysis and size-strain plot of zinc oxide nanoparticles by Williamson-Hall. *Materials Today: Proceedings*, *92*, 1334–1339. https://doi.org/ 10.1016/j.matpr.2023.05.492
14. Gul, A., Khaligh, N. G., Julkapli, N. M. (2021). Surface modification of carbon-based nanoadsorbents for the advanced wastewater treatment. *Journal of Molecular Structure*, *1235*, 130148. https://doi.org/10.1016/j.molstruc.2021.130148
15. Gurusamy, M., Thirumalaisamy, R., Karuppusamy, M., Sivanantham, G. (2025). Pistachio shell biochar as a reinforcing filler in short Turkish hemp fiber composites: a path toward sustainable materials. *Journal of Polymer Research*, *32*(4), 1–26. https://doi.org/. 10.1007/s10965-025-04338-8
16. He, Y., Wang, Y., Hu, J., Wang, K., Zhai, Y., Chen, Y.,..., Zhang, W. (2021). Photocatalytic property correlated with microstructural evolution of the biochar/ZnO composites. *Journal of Materials Research and Technology*, *11*, 1308–1321. https://doi.org/10.1016/j.jmrt.2021.01.077
17. Heo, J. W., An, L., Chen, J., Bae, J. H., Kim, Y. S. (2022). Preparation of amine-functionalized lignins for the selective adsorption of Methylene blue and Congo red. *Chemosphere*, *295*, 133815.
18. Imran, M., Ali, L., Ali, L., Wakeel, M., Siddique, M. H., Khan, Z. U. H.,..., Shahid, M. (2023). Remediation potential of biochar/copper oxide nanoparticles composite for lead-and cadmium-contaminated wastewater. *Environmental Earth Sciences, 82*(23), 574. https://doi.org/10.1007/s12665-023-11147-z

19. Jawad, N., Naife, T. M. (2022). Mathematical modeling and kinetics of removing metal ions from industrial wastewater. *Iraqi Journal of Chemical and Petroleum Engineering*, *23*(4), 59–69. https://doi.org/10.31699/IJCPE.2022.4.8
20. Li, J. (2023). Adsorption of Cd (II) and Pb (II) by Mg-modified straw biochar. *Desalination and Water Treatment, 292*, 131–140. https://doi.org/10.5004/dwt.2023.29510
21. Mitra, S., Chakraborty, A. J., Tareq, A. M., Emran, T. B., Nainu, F., Khusro, A., Simal-Gandara, J. (2022). Impact of heavy metals on the environment and human health: Novel therapeutic insights to counter the toxicity. *Journal of King Saud University-Science*, *34*(3), 101865. https://doi.org/10.1016/j.jksus.2022.101865
22. Mondal, P. (2024). Interface band alignment engineering of ZnO/Si heterojunction solar cells with high open circuit voltage. *Journal of Materials Science: Materials in Electronics*, *35*(20), 1429. https://doi.org/10.1007/s10854-024-13191-2
23. Nworie, F. S., Nwabue, F. I., Oti, W., Mbam, E. 1., Nwali, B. U. (2019). Removal of methylene blue from aqueous solution using activated rice husk biochar: Adsorption isotherms, kinetics and error analysis. *Journal of the Chilean chemical society*, *64*(1), 4365–4376. https://doi.org/10.4067/s0717-97072019000104365
24. Odumbe, E., Murunga, S., Ndiiri, J. (2023). Heavy metals in wastewater effluent: causes, effects, and removal technologies. *Trace Metals in the Environment*. https://doi.org/10.5772/intechopen.1001452
25. Padmavathy, K. S., Madhu, G., Haseena, P. V. (2016). A study on effects of pH, adsorbent dosage, time, initial concentration and adsorption isotherm study for the removal of hexavalent chromium (Cr (VI)) from wastewater by magnetite nanoparticles. *Procedia Technology, 24,* 585–594. 127. https://doi.org/10.1016/j.protcy.2016.05
26. Ramu, Y. R., Murthy, B. R. (2023). Exploring the benefits of rice husk waste: synthesis and characterization of biochar and nanobiochar for agricultural and environmental sustainability. *International Journal of Environment and Climate Change*, *13*(9), 715–725. https://doi.org/10.9734/ijecc/2023/v13i92292
27. Ramutshatsha-Makhwedzha, D., Mbaya, R., Mavhungu, M. L. (2022). Application of activated carbon banana peel coated with Al2O3-chitosan for the adsorptive removal of lead and cadmium from wastewater. *Materials*, *15*(3), 860. https://doi.org/10.3390/ma15030860
28. Saeednia, S., Iranmanesh, P., Shabani, T. (2024). Green synthesis of pistachio skin extract-mediated zinc oxide nanoparticles for photocatalytic degradation of organic dyes. *Inorganic Chemistry Research*, *8*(1), 1–7. https://doi.org/ 10.22036/J10.22036.2024.450411.1164
29. Tan, X. F., Liu, Y. G., Gu, Y. L., Xu, Y., Zeng, G. M., Hu, X. J.,..., Li, J. (2016). Biochar-based nanocomposites for the decontamination of wastewater: a review. *Bio resource technology*, *212*, 318–333. https://doi.org/10.1016/j.biortech.2016.04.093
30. Tounsadi, H., Khalidi, A., Abdennouri, M., Barka, N. (2015). Biosorption potential of Diplotaxis harra and Glebionis coronaria L. biomasses for the removal of Cd (II) and Co (II) from aqueous solutions. *Journal of Environmental Chemical Engineering*, *3*(2), 822–830. https://doi.org/10.1016/j.jece.2015.03.022
31. Vijayaraghavan, K., Rangabhashiyam, S., Ashokkumar, T., Arockiaraj, J. (2017). Assessment of samarium biosorption from aqueous solution by brown macroalga *Turbinaria conoides*. *Journal of the Taiwan Institute of Chemical Engineers*, *74*, 113–120. https://doi.org/10.1016/j.jtice.2017.02.003
32. Wattanakornsiri, A., Rattanawan, P., Sanmueng, T., Satchawan, S., Jamnongkan, T., Phuengphai, P. (2022). Local fruit peel biosorbents for lead (II) and cadmium (II) ion removal from waste aqueous solution: A kinetic and equilibrium study. *South African Journal of Chemical Engineering, 42*, 306–317. https://doi.org/10.1016/j.sajce.2022.09.008
33. Zahra, S., Bukhari, H., Qaisar, S., Sheikh, A., Amin, A. (2022). Synthesis of nanosize zinc oxide through aqueous sol–gel route in polyol medium. *BMC chemistry*, *16*(1), 104. https://doi.org/ 10.1186/s13065-022-00900-3
34. Zhang, K., Cen, R., Moavia, H., Shen, Y., Ebihara, A., Wang, G.,..., Xing, B. (2024). The role of biochar nanomaterials in the application for environmental remediation and pollution control. *Chemical Engineering Journal*, *492*, 152310. https://doi.org/10.1016/j.cej.2024.152310
35. Zhou, R., Zhang, M., Shao, S. (2022). Optimization of target biochar for the adsorption of target heavy metal ion. *Scientific reports*, *12*(1), 13662. https://doi.org/ 10.1038/s41598-022-17901-w